THE JOURNAL OF PHYSICAL CHEMISTRY B

Article

pubs.acs.org/JPCB

Bilayer Membrane Permeability of Ionic Liquid-Filled Block Copolymer Vesicles in Aqueous Solution

Zhifeng Bai,[†] Bin Zhao,[§] and Timothy P. Lodge*[,†,‡]

[†]Department of Chemistry and [‡]Department of Chemical Engineering & Materials Science, University of Minnesota, Minneapolis, Minnesota 55455, United States

[§]Department of Chemistry, University of Tennessee, Knoxville, Tennessee 37996, United States

Supporting Information

ABSTRACT: The bilayer membrane permeability of block copolymer vesicles ("polymersomes") with ionic liquid interiors dispersed in water is quantified using fluorescence quenching. Poly((1,2-butadiene)-*b*-ethylene oxide) (PB−PEO) block copolymer vesicles in water with their interiors filled with a common hydrophobic ionic liquid, 1-ethyl-3-methylimidazolium bis(trifluoromethylsulfonyl)amide, were prepared containing a hydrophobic dye, Nile Red, by intact migration of dye-encapsulated vesicles from the ionic liquid to water at room temperature. A small quencher molecule, dichloroacetamide, was added to the aqueous solution of the dye-loaded vesicles, and the permeation of the quencher passing through the membrane into the interior was determined from the fluorescence quenching kinetics. Rapid permeation of the quencher across the nanoscale membrane was observed, consistent with the high fluidity of the liquid polybutadiene membrane. Two different PB−PEO copolymers were employed, in order to vary the thickness of the solvophobic membrane. A significant increase in membrane permeability was also observed with decreasing membrane thickness, which is tentatively attributable to differences in quencher solubility in the membranes. Quantitative migration of the vesicles from the aqueous phase back to an ionic liquid phase was achieved upon heating. These microscopically heterogeneous and thermoresponsive vesicles with permeable and robust membranes have potential as recyclable nanoreactors, in which the high viscosity and capital expense of an ionic liquid reaction medium can be mitigated, while retaining the desirable features of ionic liquids as reaction media, and facile catalyst recovery.

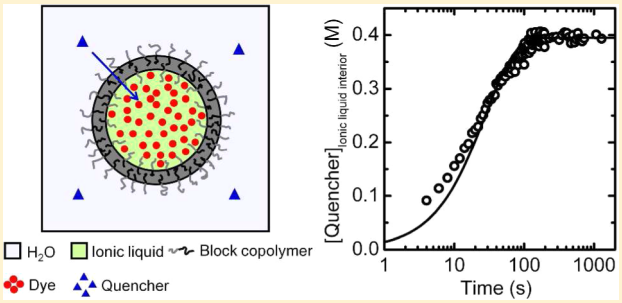

INTRODUCTION

As microcapsules enclosed by nanoscale bilayer membranes, polymer vesicles or polymersomes[1] have drawn much attention due to potential applications ranging from nanoreactors[2−4] and material fabrication templates[5] to drug delivery.[6,7] Polymer vesicles formed by self-assembly of synthetic amphiphilic block copolymers are endowed with much broader tunability than natural liposomes in terms of their membrane properties, e.g., thickness,[8,9] structure,[10−15] mechanical stability,[16,17] and chemical functionality.[18−20] Recently, we described the preparation of polymer vesicles with hydrophobic ionic liquid interiors dispersed in water, obtained by migration of polymersomes from a hydrophobic ionic liquid to an aqueous layer.[21] The polymers employed were poly((1,2-butadiene)-*b*-ethylene oxide) (PB−PEO) diblocks, where the solvophobic PB forms the membrane and the solvophilic PEO makes up the corona. This class of vesicles with different fluids inside and outside the membrane represents a novel kind of nano/microemulsion, which possesses high structural integrity as it is stabilized by a robust surfactant bilayer as compared to monolayer-stabilized emulsions. The vesicles can shuttle thermoreversibly between water and the ionic liquid, driven by the lower critical solution temperature (LCST) phase behavior of PEO in water; the same strategy has been employed to transport micellar nanocarriers[22−27] and nanoparticles.[28−30] Due to the significant promise of ionic liquids as media for reactions[31−34] and separations,[35] this microscopically heterogeneous and thermoresponsive system is of specific interest in recyclable nanoreactors. For example, although the power of ionic liquids as solvation media for organic reactions has been widely documented, they are relatively expensive and viscous. By sequestering a catalyst within the ionic-liquid filled polymersome, and dispersing into water, the economic, mixing, and mass transfer limitations of the ionic liquid can be overcome.

For many applications including nanoreactors, the transport of reagents across the vesicle membrane, expressed by permeability (p, m/s) and thickness-normalized permeation coefficient (P, m^2/s), is an important parameter.[1] Indeed, permeation of molecules across a vesicle membrane, as a model for a freestanding nanoscale film, is an interesting scientific topic in itself.[36] Due to the membrane fluidity, diffusion is more

Received: April 6, 2012
Revised: June 13, 2012
Published: July 5, 2012

rapid across a liquid membrane than a solid membrane. This was illustrated by a significant increase in permeability of protons across poly(styrene-*b*-acrylic acid) (PS−PAA) block copolymer vesicle membranes upon adding dioxane to plasticize the glassy PS membranes.[37,38] The permeability of vesicle membranes can also be tailored by introducing pores, e.g., through controlled swelling[39,40] or selective removal[41,42] of one component of two-component membranes or by installing protein channels.[43,44]

Several experimental strategies have been employed to measure membrane permeability of polymer vesicles. Permeability of solvent molecules has been determined from the rate of the swelling or shrinkage of giant polymer vesicles (typically over 10 μm in diameter) in response to an osmotic shock, as monitored by optical microscopy.[16,45] Another approach involves reactions induced by permeation of reagent across membranes into interiors containing retained catalysts and/or other reagents. If the reagents or products are spectroscopically active and the permeation is the rate-dominating step, membrane permeability of the diffusing reagents can be obtained spectroscopically.[42,46] Similarly, permeability of protons across vesicle membranes has been investigated, where pH-sensitive fluorescence dyes are encapsulated in vesicle interiors.[38,39] In addition, exchange of tracer molecules across vesicle membranes has been studied using pulsed-field-gradient nuclear magnetic resonance (PFG-NMR) spectroscopy.[47,48]

Herein, we use a simple fluorescence quenching approach to study membrane permeability of PB−PEO vesicles in water, with a common hydrophobic ionic liquid, 1-ethyl-3-methylimidazolium bis(trifluoromethylsulfonyl)amide ([EMIM][TFSA]), located in the interior. As illustrated in Figure 1, a small quencher molecule, dichloroacetamide (DCA), is added to an aqueous solution of PB−PEO vesicles with a hydrophobic fluorescent dye, Nile Red (NR), enclosed in the [EMIM][TFSA]-filled interiors. This system features exclusive partitioning of NR to the vesicle interiors, and roughly equal partitioning of DCA between water and [EMIM][TFSA]. Thus, the permeation of the quencher passing through the membrane into the interior can be determined from the quenching of the dye fluorescence. Two PB−PEO block copolymers with different PB chain lengths were employed, to prepare vesicles with different membrane thicknesses for the permeability study. Rapid (i.e., time scale of seconds) permeation of the quencher across the PB membrane was observed, consistent with the high fluidity of the liquid PB membrane (glass transition temperature $T_{g,PB,bulk} \approx -12$ °C[49]). A notable increase in the membrane permeability was observed upon decreasing the membrane thickness. Rapid permeation is desirable for possible applications of these thermoresponsive vesicles as nanoreactors. Furthermore, the fluorescence quenching via a permeation-collision-quenching mechanism[50] may serve as a model reaction to explore utilizing vesicles as nanoreactors.

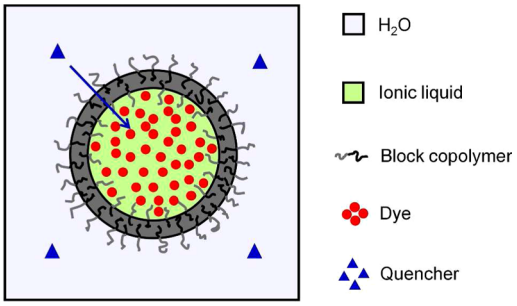

Figure 1. Schematic illustration of fluorescence quenching in the system of vesicles with ionic liquid interiors dispersed in water, adapted from ref 21.

EXPERIMENTAL SECTION

Materials. Two PB−PEO block copolymers, PB−PEO(14−4.5) and PB−PEO(6.7−2.4), were previously synthesized by Dr. Kevin Davis via sequential anionic polymerization.[51] The molecular characteristics of the polymers are summarized in Table 1; the numbers in parentheses indicate the block molar masses in kg/mol. [EMIM][TFSA] was prepared by ion exchange, as described previously.[21] NR (99%) and DCA (98%) were obtained from Acros and Aldrich, respectively, and used as received.

Table 1. Molecular Characteristics of Polymers

polymers[a]	M_{PB}[b] (kg mol^{-1})	M_{PEO}[b] (kg mol^{-1})	PDI[c]	w_{PEO}
PB−PEO(14−4.5)	14	4.5	1.03	0.25
PB−PEO(6.7−2.4)[d]	6.7	2.4	1.08	0.26

[a]90% 1,2-addition in PB as determined by ^{1}H NMR. [b]Number-average molecular weight determined by ^{1}H NMR. [c]Polydispersity index (PDI) determined by SEC. [d]Data from ref 51.

Vesicle Solution Preparation. Vesicle solutions in [EMIM][TFSA] were prepared by a thin-film protocol. A weighed amount of block copolymer was dissolved in dichloromethane in an ampule. The solvent was removed by using a gentle nitrogen purge and then drying at 50 °C in a vacuum oven (~30 mTorr) overnight, leading to a polymer thin film. A weighed amount of [EMIM][TFSA] or an [EMIM][TFSA] solution of 0.5 mM NR was added (0.5 wt % polymer), and the tube was sequentially evacuated and refilled with argon three times before it was sealed under an argon atmosphere. The polymer was dissolved upon stirring at 150 °C for 1 d. Water was added to the [EMIM][TFSA] solution of vesicles. With moderate agitation, the vesicles transferred from the ionic liquid phase to the aqueous phase in ca. 30 min at room temperature, indicated by the clear ionic liquid phase and the cloudy aqueous phase. Upon subsequent heating at 70 °C, the vesicles transferred back to the ionic liquid phase in ca. 30 min.

Laser Scanning Confocal Microscopy (LSCM). Confocal images were recorded on an Olympus FluoView FV1000 upright microscope with a Plan Apo N 60× 1.42NA immersion oil objective lens (Olympus). Fluorescence was excited using a green HeNe laser (λ_{ex} = 543 nm) and collected over 560−660 nm. The images were analyzed using Fluoview FV1000 Viewer (version 1.7a, Olympus).

Fluorescence Spectroscopy. Fluorescence spectra were measured on a Varian Cary Eclipse fluorescence spectrophotometer equipped with a temperature controller (±0.1 °C) with excitation and emission slits of 10 nm and an excitation wavelength (λ_{ex}) of 543 nm. Aqueous samples of the dye-loaded vesicles with ionic liquid interiors (0.01 wt % polymer) were filtered through 5 μm PVDF syringe filters (Millipore) prior to measurements.

dx.doi.org/10.1021/jp3033098 | J. Phys. Chem. B 2012, 116, 8282−8289

For the quenching experiments in the biphasic water/[EMIM][TFSA] system, samples were equilibrated at 30 °C prior to measurements, and fluorescence data averaged over three runs are reported. To a quartz fluorescence cell (4 × 10 mm window, 10 mm path length, Varian) fitted with a Teflon stopper, 0.6 mL of 10 μM NR in dry [EMIM][TFSA] was added and fluorescence was collected. An equal volume of water was added to the system, which was well agitated and equilibrated, and fluorescence was collected again. A weighed amount of solid DCA was then sequentially added to the biphasic system. After each addition of DCA, the system was well agitated to ensure complete dissolution of DCA and equilibration before fluorescence was collected.

For the quenching experiments in the vesicle systems, 0.6 mL aqueous solution of the transferred vesicles was added to the quartz fluorescence cell. The fluorescence of the solution was collected every 2 s at room temperature with a scanning rate of 600 nm/min from 635 to 645 nm, in which range the fluorescence peaks before and after the quenching are located. While scanning, an equal volume of a solution of 0.5 M DCA in [EMIM][TFSA]-saturated water was added using a pipet; the aqueous DCA solution was prepared by dissolving DCA in [EMIM][TFSA]-saturated water that was the aqueous phase separated from the equilibrated biphasic water/[EMIM]-[TFSA] system. To obtain good mixing, the DCA solution was injected rapidly, immediately followed by a quick aspiration and reinjection. About 4 s after the first injection, the first well-defined fluorescence trace was collected, since the addition of the DCA solution interferes with the fluorescence collection. The standard deviation of the relaxation time for the permeation of DCA across the vesicle membrane was obtained from three separate measurements.

UV−Visible Spectroscopy. Absorption spectra were obtained on a Varian Cary 100Bio UV-Visible spectrophotometer at room temperature. For the study of the NR partitioning in the biphasic water/[EMIM][TFSA] system, samples were prepared by mixing equal volumes of water and an [EMIM][TFSA] solution of 0.5 mM NR and equilibrating at room temperature. A 1 cm and a 1 mm quartz cell were used in the absorbance measurements of the aqueous phase and the [EMIM][TFSA] phase, respectively, of the biphasic water/[EMIM][TFSA] system containing the dye. The [EMIM]-[TFSA] phase was diluted gravimetrically by pure [EMIM]-[TFSA] until the absorbance was below 1. Water and [EMIM][TFSA] were used as backgrounds.

Proton Nuclear Magnetic Resonance (^{1}H NMR) Spectroscopy. ^{1}H NMR spectra were acquired on a Varian Inova 500 MHz spectrometer at room temperature. For the study of the DCA partitioning in the biphasic water/[EMIM][TFSA] system, equal volumes of an aqueous DCA solution with a concentration of 0.1 and 0.5 M ($[DCA]_{Total}$) and [EMIM]-[TFSA] were mixed and equilibrated at room temperature. A fraction of the ionic liquid phase was then taken out for ^{1}H NMR analysis. The DCA concentration in the ionic liquid phase ($[DCA]_{IL}$) was calculated using the proton integration of DCA, water and [EMIM][TFSA]. The DCA concentration in the aqueous phase ($[DCA]_{aq}$) could then be calculated from $[DCA]_{Total}$ and $[DCA]_{IL}$. For the biphasic system with higher $[DCA]_{Total}$ of 0.5 M, $[DCA]_{IL}$ was obtained from the proton integration of DCA against [EMIM][TFSA], while for the system with 0.1 M $[DCA]_{Total}$, $[DCA]_{IL}$ was obtained from the proton integration of DCA against water, and the water concentration was obtained from proton integration of water against [EMIM][TFSA]. The water concentration in the ionic liquid phase was 1.9 and 2.0 wt % for the biphasic systems with 0.1 and 0.5 M $[DCA]_{Total}$, respectively, values that are consistent with that of water-saturated [EMIM] [TFSA], ∼1.9 wt %.[52]

Dynamic Light Scattering (DLS). DLS measurements were performed on a homemade photometer outfitted with a Brookhaven BI-DS photomultiplier, a Lexel Ar^+ laser with a wavelength of 488 nm and a Brookhaven BI-9000 correlator. Measurements were acquired at 25.0 ± 0.2 °C at seven different scattering angles between 60° and 120°. [EMIM][TFSA] solutions of vesicles were diluted to 0.033 wt % using pure [EMIM][TFSA] and filtered through a 5 μm PVDF syringe filter (Millipore). The vesicles were then transferred to an aqueous phase at room temperature upon adding filtered water (0.2 μm GHP, Pall) to the diluted and filtered ionic liquid solutions.

RESULTS AND DISCUSSION

Vesicle Preparation and Characterization. Two PB−PEO block copolymers, PB−PEO(14−4.5) and PB−PEO(6.7−2.4) (see Table 1), were employed to prepare vesicles with ionic liquid interiors dispersed in water. The vesicles were initially formed in [EMIM][TFSA] by direct dissolution of a thin film of the copolymers. The vesicles then migrated spontaneously with their ionic liquid interiors to an aqueous phase upon adding water to the ionic liquid solution at room temperature, yielding vesicles with [EMIM][TFSA] in water (*i.e.*, bilayer-stabilized [EMIM][TFSA]-in-water microemulsions). The configuration of these vesicles, with a membrane formed of PB blocks and interior and exterior coronas comprising PEO chains, is thermodynamically preferred in either solvent. Due to the LCST phase behavior of PEO in water, the vesicles in the aqueous phase can quantitatively migrate back to the ionic liquid phase upon heating to 70 °C, enabling facile recovery.

Detailed characterization of the PB−PEO(14−4.5) vesicles with [EMIM][TFSA] interiors dispersed in water has been reported previously.[21] Figure 2A shows a representative laser scanning confocal microscopy (LSCM) image of the PB−PEO(6.7−2.4) vesicles in water, with NR loaded in their [EMIM][TFSA] interiors. The filled red circles clearly indicate NR is enclosed in the ionic liquid interiors of the vesicles in water. The spatial encapsulation of the dye-loaded ionic liquid pools is depicted in a series of two-dimensional (*XY*) images in the third dimension (*Z*) (Figure 2B). These LSCM images indicate that the PB−PEO(6.7−2.4) vesicles, which feature a thinner membrane than the PB−PEO(14−4.5) vesicles examined previously, are still robust and able to retain their ionic liquid interiors during the migration. Since the membrane thickness (*d*) of the PB−PEO(14−4.5) vesicles in water with either [EMIM][TFSA] or water interiors are comparable (ca. 28 nm),[21] *d* of the PB−PEO(6.7−2.4) vesicles in water with [EMIM][TFSA] interiors is expected to be ca. 18 nm, a value reported previously with water interiors.[51,53] The size of the vesicles with [EMIM][TFSA] interiors in water was also characterized using dynamic light scattering (DLS). The PB−PEO(6.7−2.4) vesicles have a mean hydrodynamic radius ($\langle R_h \rangle$) of 142 nm and a dispersity (reduced second cumulant, μ_2/Γ^2)[54] of 0.29, as compared to a $\langle R_h \rangle$ of 198 nm and a μ_2/Γ^2 of 0.44 for the PB−PEO(14−4.5) vesicles.

Fluorescence Quenching in Biphasic Water/Ionic Liquid Systems. Fluorescence quenching in the biphasic

dx.doi.org/10.1021/jp3033098 | J. Phys. Chem. B 2012, 116, 8282−8289

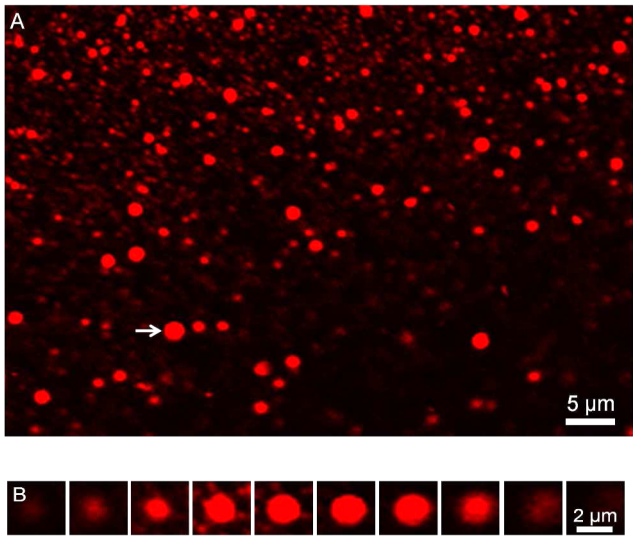

Figure 2. LSCM image of PB−PEO(6.7−2.4) vesicles in water with NR loaded in their [EMIM][TFSA] interiors (A), and *Z*-scan LSCM images of the vesicle indicated by the white arrow in A, where *XY* cross sections were taken in 0.5 μm steps in *Z* from the bottom (left) up (B).

water/[EMIM][TFSA] system was first studied as a control. The quenching was examined by analysis of the fluorescence upon consecutively adding DCA, a quencher of NR, to the biphasic water/[EMIM][TFSA] system containing NR in the ionic liquid phase. As shown in Figure 3, the NR fluorescence

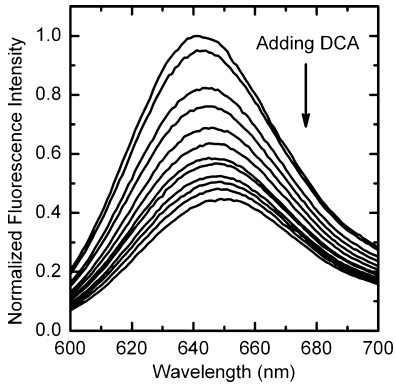

Figure 3. Fluorescence quenching of 10 μM NR in the ionic liquid phase of the biphasic water/[EMIM][TFSA] system upon consecutively adding solid DCA. The concentrations of added DCA in the ionic liquid phase are 0.007, 0.025, 0.040, 0.071, 0.101, 0.130, 0.168, 0.232, 0.301, 0.392, and 0.542 M. Data were collected in two separate experiments, with the DCA concentrations of 0.007, 0.301, 0.392, and 0.542 M from one experiment and the rest from the other.

can be effectively quenched by the addition of DCA. ^{1}H NMR spectroscopy was employed to measure the partitioning of DCA in the biphasic water/[EMIM][TFSA] system, and a partition coefficient (K_p = $[DCA]_{IL}/[DCA]_{aq}$) of 1.6 was observed,[55] where $[DCA]_{IL}$ and $[DCA]_{aq}$ are the concentrations in the ionic liquid phase and the aqueous phase, respectively. The NR partitioning in the biphasic water/[EMIM][TFSA] system was also quantified using visible spectroscopy. The hydrophobic dye partitions almost exclusively to the [EMIM][TFSA] with a K_p ($[NR]_{IL}/[NR]_{aq}$) larger than 1000; the exclusive partitioning remains after the addition of DCA to the biphasic system. In addition, as observed previously, NR also partitions almost exclusively to the [EMIM][TFSA] phase in the biphasic PB/[EMIM][TFSA] system with a K_p ($[NR]_{IL}/[NR]_{PB}$) larger than 100.[21] Thus, a system with exclusive partitioning of the dye to [EMIM]-[TFSA] against water and the PB membrane and a roughly equal partitioning of the quencher in the biphasic system is favorable for the membrane permeation study.

The fluorescence quenching of NR by DCA in the biphasic water/[EMIM][TFSA] system was then analyzed through plotting normalized fluorescence peak intensities versus $[DCA]_{IL}$ (Figure 4). According to the Stern−Volmer law,

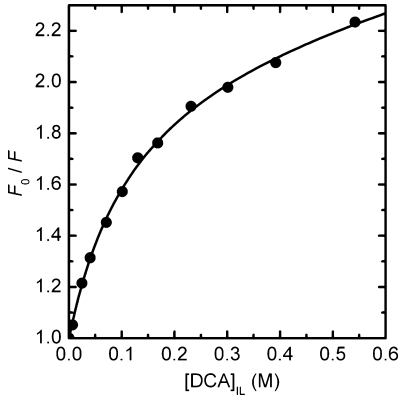

Figure 4. Stern−Volmer plot for the fluorescence quenching of NR by DCA in the biphasic water/[EMIM][TFSA] system, generated from the intensity of the emission peaks under various $[DCA]_{IL}$ in Figure 3. The solid line is a fit using eq 1 with n = 2 (R^2 = 0.999).

fluorescence quenching by dynamic bimolecular collisions can be described by $F_0/F = 1 + K_{sv}[Q]$, where F_0 and F are the fluorescence in the absence and presence of quencher, respectively, [Q] is the quencher concentration, and K_{sv} is the dynamic quenching constant. The downward curvature of the Stern−Volmer plot in Figure 4 is typically observed for fluorescence quenching in heterogeneously emitting systems, whereby the Stern−Volmer law can be modified as

$$\frac{F_0}{F} = \left(\sum_{i=1}^{n} \frac{f_i}{1 + K_{sv,i}[DCA]_{IL}} \right)^{-1} \quad (1)$$

where $K_{sv,i}$ is the dynamic quenching constant for fluorescence component *i*, and f_i is the fractional contribution of component *i* to the total fluorescence.[50] As shown in Figure 4, an excellent fit of the Stern−Volmer plot by eq 1 was achieved with a two-component fitting, suggesting the water-saturated [EMIM]-[TFSA] system is microscopically heterogeneous as probed by the dye. Indeed, according to previous experimental and computational studies, water molecules gather into microscopic water clusters/pools in wet ionic liquids,[56−59] including [EMIM][TFSA],[57] leading to microscopically heterogeneous systems that could be favorable for synthesis in ionic liquids.[32,33] The fitted results, $K_{sv,1}$ = 18 M^{-1}, f_1 = 0.56, $K_{sv,2}$ = 0.19 M^{-1}, and f_2 = 0.44, indicate that one component of NR fluorescence in the water-saturated ionic liquid phase is easily quenchable while the other is only weakly quenchable. On the other hand, it was found that fluorescence quenching of 10 μM NR in dry [EMIM][TFSA] by DCA is very weak, F_0/F(0.05 M DCA) = 1.01. This comparison suggests the easily quenchable fluorescence in the water-saturated [EMIM][TFSA] system

dx.doi.org/10.1021/jp3033098 | J. Phys. Chem. B 2012, 116, 8282−8289

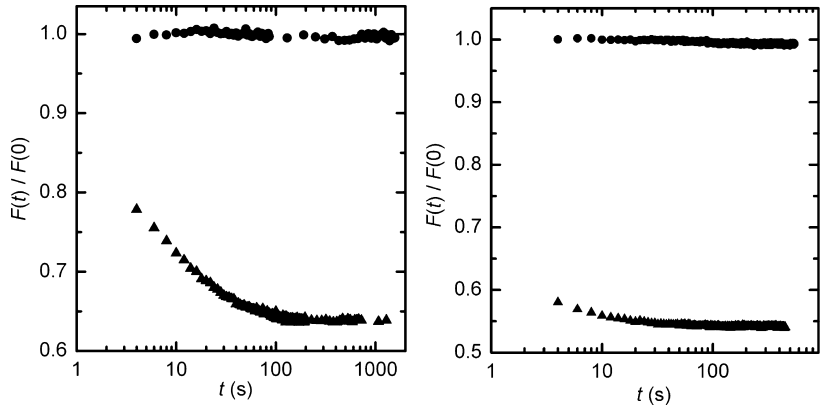

Figure 5. $F(t)/F(0)$ vs t after adding equal volume of an aqueous solution with (triangle) or without 0.5 M DCA (filled circles, as control) to an aqueous solution of the transferred PB−PEO (14−4.5) (left) and PB−PEO (6.7−2.4) (right) vesicles containing NR in the vesicle interior at 22 °C. $F(0)$ is obtained from the average of initial fluorescence in the control experiment.

arises from NR solvated in a water-rich microenvironment (water clusters/pools), while the weakly quenchable fluorescence comes from NR solvated in a microenvironment with relatively low water content.[60]

Fluorescence Quenching in Vesicle Systems. The NR/DCA fluorescence quenching pair was employed to study the membrane permeability of the PB−PEO (14−4.5) and PB−PEO (6.7−2.4) vesicles with ionic liquid interiors dispersed in water. An equal volume of 0.5 M aqueous DCA solution was well mixed with the dye-loaded vesicles in water.[61] DLS was used to characterize the vesicles after mixing, revealing that the size and size distribution of the vesicles do not change, e.g., a $\langle R_h \rangle$ of 145 nm and a μ_2/Γ^2 of 0.30 for the PB−PEO (6.7−2.4) vesicles. Moreover, LSCM analysis indicated NR is still enclosed in the vesicle interiors after mixing (see Supporting Information). These results are consistent with the stability and robustness of the PB−PEO vesicles. Figure 5 shows the time evolution of the fluorescence quenching for the PB−PEO (14−4.5) and PB−PEO (6.7−2.4) vesicles. The fluorescence quenching for the PB−PEO(14−4.5) vesicles with a thicker membrane features an exponential decay to a steady value in about 2 min, while that for the PB−PEO(6.7−2.4) vesicles is rather rapid so that only the late portion of the quenching was captured by the current method.[62]

Membrane permeability of the vesicles can be extracted from the fluorescence quenching. Figure 6 shows the time evolution of $[DCA]_{IL}$ in the vesicle interiors derived from the time evolution of fluorescence quenching in the vesicle system and the relation between F_0/F and $[DCA]_{IL}$ obtained from the fluorescence quenching in the biphasic water/ionic liquid system in the preceding section (see Supporting Information for further details). The exponential-like time evolution of $[DCA]_{IL}$ was then fitted by an equation derived from a permeation model previously reported for common vesicle systems (see the Appendix)[39,63]

$$[DCA]_{IL}(t) = K_p[DCA]_{aq}(1 - e^{-t/\tau}) \quad (2)$$

where t is time and τ is the relaxation time for the permeation of DCA across the membrane. Note that $[DCA]_{aq}$ is essentially constant during the permeation due to the large volume ratio of the aqueous matrix to the vesicular ionic liquid interiors and the roughly equal partitioning of DCA in water and the ionic liquid. As shown by the fitting in Figure 6, the simple model agrees reasonably well with the experimental results, especially for the

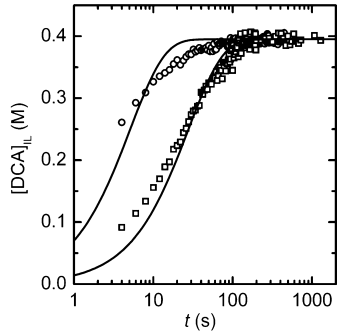

Figure 6. $[DCA]_{IL}$ vs t after adding equal volume of a 0.5 M DCA aqueous solution to an aqueous solution of the transferred PB−PEO (14−4.5) (square) and PB−PEO (6.7−2.4) (circle) vesicles containing NR in the vesicle interior. The solid lines are fits using eq 2 with R^2 of 0.95 and 0.69 for the PB−PEO (14−4.5) and PB−PEO (6.7−2.4) vesicles, respectively.

PB−PEO (14−4.5) vesicle system. The fitted τ for the permeation of DCA across the PB−PEO (14−4.5) and PB−PEO (6.7−2.4) vesicle membranes is 26 ± 3 and 4 ± 1.5 s, respectively.[64] The permeability (p) and permeation coefficient (P) of DCA across the vesicle membrane can thus be calculated from

$$\tau = \frac{R_h}{3p} = \frac{R_h d}{3P} \quad (3)$$

yielding a p of 2.6 and 12 nm/s and a P of 71 and 210 nm^2/s for the PB−PEO (14−4.5) and PB−PEO (6.7−2.4) vesicles, respectively. As each vesicle contributes independently to the fluorescence signal, with $\tau \approx R_h$, we use the mean R_h in eq 3. Remarkably, a decrease in d from 28 to 18 nm boosts p and P by a factor of almost 5 and 3, respectively.

Studies on membrane permeability of polymer vesicles with varying membrane thickness are limited. Mayer and co-workers reported that P of a 200 g/mol PEO oligomer across the membranes of poly(2-vinylpyridine-*b*-ethylene oxide) vesicles in water decreases by a factor of 2 with an increase of the membrane thickness from 9 to 15 nm.[48] However, Battaglia, Ryan and Tomas found that P of 5,5′-dithiobis-2-nitrobenzoic acid (DTNB) across the membranes of PBO−PEO and PEO−PBO−PEO vesicles in water appeared to be almost independent of the membrane thickness over a range from 2.4 to 7.6 nm.[46] In principle, the d-normalized P is proportional

dx.doi.org/10.1021/jp3033098 | J. Phys. Chem. B 2012, 116, 8282−8289

Table 2. Permeation Coefficient of Various Vesicle Membranes

membrane	liposomes			PEE−PEO	PB−PEO	PB−PEO
d (nm)		~3		8	9	18/28
diffuser	water	glycerol, glucose, urea	Na^+, K^+, Cl^-	water	water	DCA
P (nm^2/s)	$2 - 30 \times 10^4$	$2 - 90$	$3 - 300 \times 10^{-5}$	2.0×10^4	2.8×10^4	210/71
membrane	PS−PAA	PBO−PEO/PEO−PBO−PEO		PMOXA−PDMS−PMOXA		PDMS-*g*-PEO
d (nm)	33	2.4 − 7.6		~25		5
diffuser	proton	DTNB		water		water
P (nm^2/s)	$1.1 \times 10^{-4} - 1.2^a$	~2		2×10^4		1.4×10^5

[a]In aqueous solutions with 7−40 wt % dioxane.

to the solubility (S) and diffusion coefficient (D) of the permeating molecules in the polymer membrane.[65] As simply suggested by the Flory−Huggins theory, solubility of small molecules in a polymer matrix decreases with increasing polymer chain length, as also observed experimentally.[66−69] For example, a decrease by about a factor of 3 in solubility of two alkylimidazolium-based ionic liquids in PEO was observed upon changing the PEO molecular weight from 2 to 3.4 kDa.[68] Likewise, the two solvent molecules, water and [EMIM]-[TFSA], in the current system likely have solubility difference in the two polymer membranes, which may increase the difference of DCA solubility in the membranes. As for diffusion of small molecules in a polymer matrix, D is inversely dependent on the friction coefficient between the small molecules and the polymer.[70] The small molecule friction coefficient is relatively independent of polymer chain length. For nanoscale polymeric films, decrease in film thickness may lower T_g and enhance fluidity of the overall films due to the higher mobility of their free surface, e.g., for polystyrene.[71] However, Discher and co-workers suggested that T_g of PB-like polyethylethylene (PEE) vesicle membrane (d = 8 nm) and bulk/melt are equivalent.[72] Thus, we expect that D of DCA in the two liquid PB membranes does not significantly differ, and hence the difference in P of the two membranes presumably arises primarily from the d dependence of S.

It is worthwhile to compare the membrane permeability observed here with those reported for other systems. As listed in Table 2, for permeation across liposome membranes, values of P of neutral polar molecules, such as glucose, glycerol, and urea, are comparable to those of DCA across the PB−PEO vesicle membranes.[65,73] Permeation of small ions, such as Na^+, K^+, and Cl^-, is much slower, while water (though polar) can permeate more rapidly.[65,73] For polymersomes, high permeability of water was also observed in liquid PEE−PEO,[16] PB−PEO,[45] and poly(2-methyloxazoline-*b*-dimethylsiloxane-*b*-2-methyloxazoline) (PMOXA−PDMS−PMOXA)[74] and PDMS-*graft*-PEO[45] vesicle membranes. The 7-fold difference in P of water across the two PDMS membranes reflects the influence of polymer structure and membrane thickness on membrane permeability. Permeation of protons across a glassy PS membrane is extremely slow, but can be increased through plasticization of the membrane using hexane.[37,38] Ionic and larger DTNB has a moderate P in PBO−PEO and PEO−PBO−PEO vesicle membranes, although the membranes are less hydrophobic.[46] The relatively high P of DCA across the PB membranes is consistent with the fluidity of the liquid PB membrane and the small size of the neutral and relatively nonpolar DCA molecule.

SUMMARY

We have prepared permeable bilayer stabilized microemulsions of PB−PEO polymer vesicles with [EMIM][TFSA] interiors dispersed in water. The membrane permeability of the vesicles was investigated using a simple fluorescence quenching protocol, where a small quencher molecule (DCA) diffuses from the aqueous matrix crossing the PB membrane into the vesicular ionic liquid to quench the enclosed hydrophobic NR dye. If appropriate quencher and dye are chosen, this facile method could also be employed to study permeability in different vesicle systems. Vesicles with different membrane thicknesses, self-assembled from two PB−PEO block copolymers with different PB chain length, were employed to study the membrane permeability. It was found that DCA can permeate rapidly across the nanoscale PB membrane, consistent with the high fluidity of the liquid PB membrane. The permeability exhibits a significant dependence on membrane thickness, indicating a way to tune the membrane permeability. The microscopically heterogeneous and thermoresponsive vesicles with permeable (liquid) and robust (relatively thick) membranes hold promise as recyclable nanoreactors. The fluorescence quenching in the vesicle system with a permeation-collision-quenching mechanism mimics a chemical reaction utilizing the vesicles as nanoreactors.

APPENDIX

A model for the permeability of DCA across the vesicle membranes was developed using a previously reported method.[39,63] In a short delay time (∂t) during the permeation, the amount of DCA across the membrane into the vesicle interior can be written as

$$V_{IL}\partial[DCA]_{IL}(t) = \frac{Sp}{2}(K_p[DCA]_{aq}(t) - [DCA]_{IL}(t))\partial t \quad (A1)$$

where $[DCA]_{aq}(t)$ and $[DCA]_{IL}(t)$ are the concentration of DCA in the aqueous matrix and the ionic liquid interiors, respectively, at a time t, S is the sum of the outer and inner surface area of the vesicle membrane, and p is the permeability of DCA across the vesicle membrane. In the limit of $V_{aq} \gg V_{IL}$, $[DCA]_{aq}(t)$ is a constant as described above, so equation A1 can take the form of

$$V_{IL}\partial[DCA]_{IL}(t) = \frac{Sp}{2}(K_p[DCA]_{aq} - [DCA]_{IL}(t))\partial t \quad (A2)$$

which can be written in a differential form

dx.doi.org/10.1021/jp3033098 | J. Phys. Chem. B 2012, 116, 8282−8289

$$\frac{d\left(\frac{[DCA]_{IL}(t)}{K_p[DCA]_{aq}}\right)}{dt} = \frac{Sp}{2V_{IL}}\left(1 - \frac{[DCA]_{IL}(t)}{K_p[DCA]_{aq}}\right) \quad (A3)$$

Equation A3 can be resolved as a single exponential relaxation

$$[DCA]_{IL}(t) = K_p[DCA]_{aq} + ([DCA]_{IL}(0) - K_p[DCA]_{aq})\, e^{-t/\tau} \quad (A4)$$

where τ is the relaxation time for the permeation of DCA across the membrane, given by

$$\tau = \frac{2V_{IL}}{Sp} \quad (A5)$$

Due to the relatively short corona block compared to the vesicle size, the outer radius of the vesicles is approximately equal to R_h of the vesicles. Then, p can be written as

$$p = \frac{2V_{IL}}{S\tau} = \frac{2(R_h - d)^3}{3\tau({R_h}^2 + (R_h - d)^2)} \quad (A6)$$

and simplified in the limit of $R_h \gg d$ as

$$p = \frac{R_h}{3\tau} \quad (A7)$$

P of DCA across the PB membrane can also be calculated using

$$P = pd \quad (A8)$$

The exponential-based permeation model was then applied to extract p and P of DCA across the vesicle membrane from the time evolution of $[DCA]_{IL}$ in the vesicle interior.

■ ASSOCIATED CONTENT

Supporting Information

DLS results of the vesicles with [EMIM][TFSA] interiors in water and derivation of the time evolution of $[DCA]_{IL}$ in the vesicle interior from the time evolution of fluorescence quenching using the relation between F_0/F and $[DCA]_{IL}$ obtained from the fluorescence quenching in the biphasic water/ionic liquid system. This material is available free of charge via the Internet at http://pubs.acs.org.

■ AUTHOR INFORMATION

Corresponding Author

*E-mail: lodge@umn.edu.

Notes

The authors declare no competing financial interest.

■ ACKNOWLEDGMENTS

This work was supported by the National Science Foundation through Award DMR-0804197 and by the Doctoral Dissertation Fellowship of the University of Minnesota (Z.B.). We acknowledge Dr. Kevin Davis for generous supply of the block copolymers, Prof. Valerie Pierre for providing access to the UV−visible and fluorescence spectrophotometers, and Dr. Jian Qin, Dr. Brad H. Jones, Yuanyan Gu, and Soonyong So for helpful discussion.

■ REFERENCES

(1) Discher, D. E.; Eisenberg, A. *Science* **2002**, *297*, 967−973.
(2) Vriezema, D. M.; Aragones, M. C.; Elemans, J. A. A. W.; Cornelissen, J. J. L. M.; Rowan, A. E.; Nolte, R. J. M. *Chem. Rev.* **2005**, *105*, 1445−1489.
(3) Kita-Tokarczyk, K.; Grumelard, J.; Haefele, T.; Meier, W. *Polymer* **2005**, *46*, 3540−3563.
(4) Kim, K. T.; Meeuwissen, S. A.; Nolte, R. J. M.; van Hest, J. C. M. *Nanoscale* **2010**, *2*, 844−858.
(5) Hamley, I. W. *Angew. Chem., Int. Ed.* **2003**, *42*, 1692−1712.
(6) Discher, D. E.; Ahmed, F. *Annu. Rev. Biomed. Eng.* **2006**, *8*, 323−341.
(7) Meng, F.; Zhong, Z.; Feijen, J. *Biomacromolecules* **2009**, *10*, 197−209.
(8) Bermudez, H.; Brannan, A. K.; Hammer, D. A.; Bates, F. S.; Discher, D. E. *Macromolecules* **2002**, *35*, 8203−8208.
(9) Wang, W.; McConaghy, A. M.; Tetley, L.; Uchegbu, I. F. *Langmuir* **2001**, *17*, 631−636.
(10) Zhang, L. F.; Eisenberg, A. *Science* **1995**, *268*, 1728−1731.
(11) van Hest, J. C. M.; Delnoye, D. A. P.; Baars, M. W. P. L.; van Genderen, M. H. P.; Meijer, E. W. *Science* **1995**, *268*, 1592−1595.
(12) Yu, G. R.; Eisenberg, A. *Macromolecules* **1998**, *31*, 5546−5549.
(13) Saito, N.; Liu, C.; Lodge, T. P.; Hillmyer, M. A. *ACS Nano* **2010**, *4*, 1907−1912.
(14) Percec, V.; et al. *Science* **2010**, *328*, 1009−1014.
(15) LoPresti, C.; Massignani, M.; Fernyhough, C.; Blanazs, A.; Ryan, A. J.; Madsen, J.; Warren, N. J.; Armes, S. P.; Lewis, A. L.; Chirasatitsin, S.; Engler, A. J.; Battaglia, G. *ACS Nano* **2011**, *5*, 1775−1784.
(16) Discher, B. M.; Won, Y. Y.; Ege, D. S.; Lee, J. C. M.; Bates, F. S.; Discher, D. E.; Hammer, D. A. *Science* **1999**, *284*, 1143−1146.
(17) Aranda-Espinoza, H.; Bermudez, H.; Bates, F. S.; Discher, D. E. *Phys. Rev. Lett.* **2001**, *87*, 208301.
(18) Antonietti, M.; Forster, S. *Adv. Mater.* **2003**, *15*, 1323−1333.
(19) Blanazs, A.; Armes, S. P.; Ryan, A. J. *Macromol. Rapid Commun.* **2009**, *30*, 267−277.
(20) Hawker, C. J.; Wooley, K. L. *Science* **2005**, *309*, 1200−1205.
(21) Bai, Z.; Lodge, T. P. *J. Am. Chem. Soc.* **2010**, *132*, 16265−16270.
(22) He, Y.; Lodge, T. P. *J. Am. Chem. Soc.* **2006**, *128*, 12666−12667.
(23) Bai, Z.; He, Y.; Lodge, T. P. *Langmuir* **2008**, *24*, 5284−5290.
(24) Bai, Z.; He, Y.; Young, N. P.; Lodge, T. P. *Macromolecules* **2008**, *41*, 6615−6617.
(25) Bai, Z.; Lodge, T. P. *J. Phys. Chem. B* **2009**, *113*, 14151−14157.
(26) Bai, Z.; Lodge, T. P. *Langmuir* **2010**, *26*, 8887−8892.
(27) Guerrero-Sanchez, C.; Gohy, J. F.; D'Haese, C.; Thijs, H.; Hoogenboom, R.; Schubert, U. S. *Chem. Commun.* **2008**, 2753−2755.
(28) Li, D.; Zhao, B. *Langmuir* **2007**, *23*, 2208−2217.
(29) Horton, J. M.; Bai, Z.; Jiang, X.; Li, D.; Lodge, T. P.; Zhao, B. *Langmuir* **2011**, *27*, 2019−2027.
(30) Horton, J. M.; Bao, C.; Bai, Z.; Lodge, T. P.; Zhao, B. *Langmuir* **2011**, *27*, 13324−13334.
(31) Dupont, J.; de Souza, R. F.; Suarez, P. A. Z. *Chem. Rev.* **2002**, *102*, 3667−3692.
(32) Parvulescu, V. I.; Hardacre, C. *Chem. Rev.* **2007**, *107*, 2615−2665.
(33) van Rantwijk, F.; Sheldon, R. A. *Chem. Rev.* **2007**, *107*, 2757−2785.
(34) Hallett, J. P.; Welton, T. *Chem. Rev.* **2011**, *111*, 3508−3576.
(35) Han, X.; Armstrong, D. W. *Acc. Chem. Res.* **2007**, *40*, 1079−1086.
(36) Paeng, K.; Swallen, S. F.; Ediger, M. D. *J. Am. Chem. Soc.* **2011**, *133*, 8444−8447.
(37) Choucair, A.; Soo, P. L.; Eisenberg, A. *Langmuir* **2005**, *21*, 9308−9313.
(38) Wu, J.; Eisenberg, A. *J. Am. Chem. Soc.* **2006**, *128*, 2880−2884.
(39) Yu, S.; Azzam, T.; Rouiller, I.; Eisenberg, A. *J. Am. Chem. Soc.* **2009**, *131*, 10557−10566.
(40) Du, J. Z.; Armes, S. P. *J. Am. Chem. Soc.* **2005**, *127*, 12800−12801.
(41) Ahmed, F.; Discher, D. E. *J. Controlled Release* **2004**, *96*, 37−53.

(42) Kim, K. T.; Cornelissen, J. J. L. M.; Nolte, R. J. M.; van Hest, J. C. M. *Adv. Mater.* **2009**, *21*, 2787−2791.
(43) Nardin, C.; Thoeni, S.; Widmer, J.; Winterhalter, M.; Meier, W. *Chem. Commun.* **2000**, 1433−1434.
(44) Sauer, M.; Haefele, T.; Graff, A.; Nardin, C.; Meier, W. *Chem. Commun.* **2001**, 2452−2453.
(45) Carlsen, A.; Glaser, N.; Le Meins, J. F.; Lecommandoux, S. *Langmuir* **2011**, *27*, 4884−4890.
(46) Battaglia, G.; Ryan, A. J.; Tomas, S. *Langmuir* **2006**, *22*, 4910−4913.
(47) Leson, A.; Filiz, V.; Förster, S.; Mayer, C. *Chem. Phys. Lett.* **2007**, *444*, 268−272.
(48) Leson, A.; Hauschild, S.; Rank, A.; Neub, A.; Schubert, R.; Föster, S.; Mayer, C. *Small* **2007**, *3*, 1074−1083.
(49) Ferry, J. D. *Viscoelastic Properties of Polymers*, 3rd ed.; Wiley: New York, 1980.
(50) Eftink, M. R.; Ghiron, C. A. *Anal. Biochem.* **1981**, *114*, 199−227.
(51) Davis, K. P. Ph. D. Thesis, University of Minnesota, 2009.
(52) Freire, M. G.; Carvalho, P. J.; Gardas, R. L.; Marrucho, I. M.; Santos, L. M. N. B. F.; Coutinho, J. A. P. *J. Phys. Chem. B* **2008**, *112*, 1604−1610.
(53) Davis, K. P.; Lodge, T. P.; Bates, F. S. *Macromolecules* **2008**, *41*, 8289−8291.
(54) A measure of the width of the micelle size distribution. See Koppel, D. E. *J. Chem. Phys.* **1972**, *57*, 4814−4820.
(55) An average of K_p (1.51 and 1.65) of 0.1 and 0.5 M DCA, respectively, in the biphasic water/[EMIM][TFSA] system. See the Experimental Section for details.
(56) Bhargava, B. L.; Yasaka, Y.; Klein, M. L. *Chem. Commun.* **2011**, *47*, 6228−6241.
(57) Porter, A. R.; Liem, S. Y.; Popelier, P. L. A. *Phys. Chem. Chem. Phys.* **2008**, *10*, 4240−4248.
(58) Sieffert, N.; Wipff, G. *J. Phys. Chem. B* **2006**, *110*, 13076−13085.
(59) Rollet, A. L.; Porion, P.; Vaultier, M.; Billard, I.; Deschamps, M.; Bessada, C.; Jouvensal, L. *J. Phys. Chem. B* **2007**, *111*, 11888−11891.
(60) It should be noted that the ratio of f_1 and f_2 reflects NR fluorescence partitioning instead of NR partitioning, as the quantum yield of NR is sensitive to its solvation environment. Kucherak, O. A.; Oncul, S.; Darwich, Z.; Yushchenko, D. A.; Arntz, Y.; Didier, P.; Mely, Y.; Klymchenko, A. S. *J. Am. Chem. Soc.* **2010**, *132*, 4907−4916.
(61) Since the aqueous vesicle solution prepared by the vesicle transfer from [EMIM][TFSA] to water is saturated with [EMIM][TFSA], the aqueous DCA solution was prepared using [EMIM][TFSA]-saturated water to match the [EMIM][TFSA] concentration in the aqueous matrix before and after mixing, which prevents possible leakage of the enclosed [EMIM][TFSA] after mixing.
(62) It should be noted that the fluorescence quenching is much faster than the sedimentation of the heavier vesicles with ionic liquid interiors in water. The speed of sedimentation (ν) can be estimated from $\nu = (2Rg(\rho_1 - \rho_2)/9\eta)^{0.5}$, where R is the vesicle radius, g is the acceleration of gravity, η is the viscosity of water, and ρ_1 and ρ_2 are the densities of the water and [EMIM][TFSA], respectively (e.g., ν is $\sim 3 \times 10^{-7}$ m/s for a vesicle with a diameter of 1 μm).
(63) Sato, T.; Kijima, M.; Shiga, Y.; Yonezawa., Y. *Langmuir* **1991**, *7*, 2330−2335.
(64) A comparable τ of 5 ± 1.5 s was observed for the quenching experiment of the PB−PEO (6.7−2.4) vesicles with a lower DCA concentration, i.e., 0.29 M aqueous DCA solution mixed with the dye-loaded vesicle solution, which suggests insensitive dependence of τ on DCA concentration.
(65) Förster, S.; Borchert, K. Polymer Vesicles. In *Encyclopedia of Polymer Science and Technology*; John Wiley & Sons: New York, 2005.
(66) Bae, Y. C.; Lambert, S. M.; Soane, D. S.; Prausnitz, J. M. *Macromolecules* **1991**, *24*, 4403−4407.
(67) Tsuda, R.; Kodama, K.; Ueki, T.; Kokubo, H.; Imabayashi, S.; Watanabe, M. *Chem. Commun.* **2008**, 4939−4941.
(68) Rodriguez, H.; Francisco, M.; Rahman, M.; Sun, N.; Rogers, R. D. *Phys. Chem. Chem. Phys.* **2009**, *11*, 10916−10922.
(69) Lee, H. N.; Lodge, T. P. *J. Phys. Chem. Lett.* **2010**, *1*, 1962−1966.
(70) Curtiss, C. F.; Bird, R. B. *Proc. Natl. Acad. Sci. U.S.A.* **1996**, *93*, 7440−7445.
(71) Mattsson, J.; Forrest, J. A.; Boerjesson, L. *Phys. Rev. E* **2000**, *62*, 5187−5200.
(72) Lee, J. C. M.; Santore, M.; Bates, F. S.; Discher, D. E. *Macromolecules* **2002**, *35*, 323−326.
(73) Stryer, L. *Biochemistry*, 3rd ed.; W. H. Freeman and Co.: San Francisco, CA, 1988.
(74) Kumar, M.; Grzelakowski, M.; Zilles, J.; Clark, M.; Meier, W. *Proc. Natl. Acad. Sci. U.S.A.* **2007**, *104*, 20719−20724.